J. Amer. Soc. Hort. Sci. 146(1):3–13. 2021. https://doi.org/10.21273/JASHS05002-20

Far-red Fraction: An Improved Metric for Characterizing Phytochrome Effects on Morphology

Paul Kusuma and Bruce Bugbee
Crop Physiology Laboratory, Utah State University, Logan, UT 84341

Additional index words. photobiology, phytochrome photoequilibrium, R:FR ratio, total phytochrome

Abstract. **Phytochrome, a well-studied photoreceptor in plants, primarily absorbs in the red (R) and far-red (FR) regions and is responsible for the perception of shade and subsequent morphological responses. Experiments performed in controlled environments have widely used the R:FR ratio to simulate the natural environment and used phytochrome photoequilibrium (PPE) to simulate the activity of phytochrome. We review why PPE may be an unreliable metric, including differences in weighting factors, multiple phytochromes, nonphotochemical reversions, intermediates, variations in the total pool of phytochrome, and screening by other pigments. We suggest that environmental signals based on R and FR photon fluxes are a better predictor of plant shape than the more complex PPE model. However, the R:FR ratio is nonintuitive and can approach infinity under electric lights, which makes it difficult to extrapolate from studies in controlled environments to the field. Here we describe an improved metric: the FR fraction (FR/R + FR) with a range from 0 to 1. This is a more intuitive metric both under electric lights and in the field compared with other ratios because it is positively correlated with phytochrome-mediated morphological responses. We demonstrate the reliability of this new metric by reanalyzing previously published data.**

Many photobiological studies are conducted under electric lights to better understand basic plant responses. In this review, we discuss the history, derivation, and limitations of two of the common metrics that are used to interpret photobiological responses: phytochrome photoequilibrium (PPE) and the R:FR ratio. Issues with these metrics are exacerbated under light-emitting diodes (LEDs), which are important to photobiology because of their narrow bandwidth. Furthermore, the high efficiency output of LEDs has made them a prominent addition to controlled environment agriculture (Kusuma et al., 2020). In these plant factories, plant morphology can be manipulated by the specific choice of LEDs, but first it is vital to develop proper metrics to predict responses.

In this review, we describe an improved metric called the FR fraction (FR/R+FR), which a ranges from 0 to 1. This is a more intuitive metric both under electric and natural conditions compared with other ratios because it is positively correlated with phytochrome-mediated morphological responses like stem elongation. We demonstrate the reliability of this new metric by reanalyzing previously published data.

Early Phytochrome Research

Seventy years ago, the discovery of phytochrome by Borthwick et al. (1952) and initial extraction by Butler et al. (1959) led to a photobiological focus on the R and FR regions of the electromagnetic spectrum. Early studies were more focused on *how* phytochrome-mediated responses occurred, like wavelength sensitivity, signaling partners, and time dependencies; but there was little focus on understanding *why* these responses happened (evolutionary and ecological perspectives). Researchers eventually began considering the ecological implications realizing, *"Beneath the forest canopy the intensity of radiation is decreased but the region of 730 nm is enhanced relative to 660 nm because of the filtering action of chlorophyll"* (Hendricks and Borthwick, 1963).

This led to studies in the natural environment (Kasperbauer, 1971; Taylorson and Borthwick, 1969) as opposed to laboratory settings with electric lighting experiments including pulses, flip-flops (following R pulses with FR pulses to reverse the response) and monochromatic light. The focus remained on R and FR because the two forms of phytochrome, P_r and P_{fr}, had absorbance peaks in these regions (Butler et al., 1964), and the R:FR ratio became well established as an indicator of the degree of shade (Cumming, 1963; Holmes and Smith, 1975, 1977a, 1977b).

Phytochrome responses, especially stem-extension rate and stem length, are often shown to be log-linearly or linearly correlated with the ratio of active phytochrome (P_{fr}) to total phytochrome (P_{total}), where $P_{total} = P_r + P_{fr}$ (Kalaitzoglou et al., 2019; Morgan and Smith, 1976, 1978, 1979; Park and Runkle, 2017, 2018, 2019). This ratio is referred to as phytochrome photoequilibrium [PPE (also called the phytochrome photostationary state, PSS)] and was popularized by H. Smith for predicting shade-avoidance responses. Smith credits K.M. Hartmann for the model of active to total phytochrome as the appropriate method for predicting phytochrome action (Hartmann, 1966; Smith, 1973).

Therefore, two metrics for predicting phytochrome responses have evolved: PPE and the R:FR ratio. Here we discuss problems with both metrics and propose a new metric.

Received for publication 2 Oct. 2020. Accepted for publication 2 Nov. 2020. Published online 8 December 2020.
This work was supported by the Utah Agricultural Experiment Station, Utah State University (journal paper number 9365); the U.S. Department of Agriculture-National Institute of Food and Agriculture-Specialty Crop Research Initiative (grant number 2018-51181-28365) (LAMP Project) NASA-Center for the Utilization of Biological Engineering in Space (grant number NNX17AJ31G).
Mention of a trademark, proprietary product, or vendor does not constitute a guarantee or warranty of the product and does not imply its approval to the exclusion of other products or vendors that also may be suitable.
P.K. is the corresponding author. E-mail: paul.kusuma@aggiemail.usu.edu.

Measurement of the Two Forms of Phytochrome

Phytochrome photoequilibrium can be estimated with a model (PPE_e) or measured directly in chlorophyll-deficient tissue (PPE_m). In chlorophyll-deficient tissue the relative amounts of the two forms of phytochrome can be measured directly in vivo using a specialized dual-wavelength spectrophotometer. There are two methods for measuring PPE_m with this technique (Dooskin and Mancinelli, 1968; Klose, 2019; Lamparter et al., 1994), but the method used by Smith and Holmes (1977) is described by Klein et al. (1967) and more recently, Klose (2019). Briefly, both methods measure the change in the difference in absorbance between two wavelength on exposure to R or FR, and the two techniques differ in the wavelengths that they measure. One measures the difference in absorbance between 660 and 730 nm, whereas the other (Smith and Holmes, 1977) measures the difference between 730 and 800 nm. The former provides a larger signal, whereas the latter reduces error caused by chlorophyll. We describe the theory behind the more commonly used technique in Supplemental Material 1. It is important to note that although we call this a measurement of P_{fr}/P_{total}, it is still an estimate.

Estimating the Equilibrium between the Two Forms (PPE_e)

PPE_e is calculated from the spectral photon distribution (SPD) and weighting factors for both P_r and P_{fr} across the biologically active wavelengths (300 to 800 nm). These weighting factors, called photochemical/photoconversion cross-sections, quantum efficiencies, or photoconversion coefficients can be derived from absorbance spectra, extinction coefficients and quantum yields of P_r to P_{fr} or P_{fr} to P_r conversion. These values are presented in at least 10 studies (Butler et al., 1964; Gardner and Graceffo, 1982; Kelly and Lagarias, 1985; Lagarias et al., 1987; Mancinelli, 1986, 1988a, 1994; Pratt and Briggs, 1966; Sager et al., 1988; Seyfried and Schäfer, 1985; Vierstra and Quail, 1983a, 1983b). The weighting factors from Sager et al. (1988) have been the most widely used in horticulture, but are not necessarily a reference standard. PPE_e has been widely adopted.

Differences in Estimated and Measured PPE

Gardner and Graceffo (1982), Sager et al. (1988), and Mancinelli (1988b) all report comparisons between PPE_m and PPE_e. Figure 1 shows this comparison. Gardner and Graceffo (1982) measured and estimated P_{fr}/P_{total} in vivo, Sager et al. (1988) measured and estimated P_{fr}/P_{total} in vitro, and Mancinelli (1988b) measured P_{fr}/P_{total} in vivo, but used estimations from in vitro data. In addition, Gardner and Graceffo (1982) assumed a P_{fr}/P_{total} under red actinic photons to be 0.8, Sager et al. (1988) assumed it to be 0.89, and Mancinelli (1988b) assumed it to be 0.876. Mancinelli (1988b) used the approach to equilibrium analysis data from Kelly and Lagarias (1985). Notice that data do not perfectly fall on the 1:1 line.

Issues with P_{fr}/P_{total} as a Model to Predict Morphology

Studies on the structure of phytochrome, nuclear localization, and genetic regulating partners have strongly indicated that P_{fr} is the active form of phytochrome (Chen and Chory, 2011; Legris et al., 2019), although some studies have specifically implicated that the P_{fr}-P_{fr} homodimer is the active form, whereas both the P_r-P_r homodimer and the P_r-P_{fr} heterodimer are inactive (Klose et al., 2015). It is often assumed that P_{fr}/P_{total} is a proxy for the concentration of P_{fr} because it is assumed that the total pool of phytochrome is relatively constant (Casal, 2012; Kilsby and Johnson, 1982; Kozma-Bognár et al., 1999; Park and Runkle, 2017). Many studies have found that P_{fr}/P_{total} is correlated with morphological responses (Kalaitzoglou et al., 2019; Morgan and Smith, 1976, 1978, 1979; Park and Runkle, 2017, 2018, 2019), and it has become common to report PPE_e in photobiology studies even if they are not investigating the effects of R and FR (Hernández and Kubota, 2016; Johnson et al., 2020; Kim et al., 2019; Meng et al., 2019; Poel and Runkle, 2017). These correlations between P_{fr}/P_{total} and morphology strongly imply the role of phytochrome in these responses, but the correlations in these studies would be equally predicted by a relationship using R and FR because these are the only wavelengths that varied in the studies. In cases in which other wavelengths vary, the results have been graphed separately (Park and Runkle, 2019).

The ratio of P_{fr}/P_{total} is often thought to fully explain phytochrome activity and subsequent developmental responses, but there are multiple problems with its use.

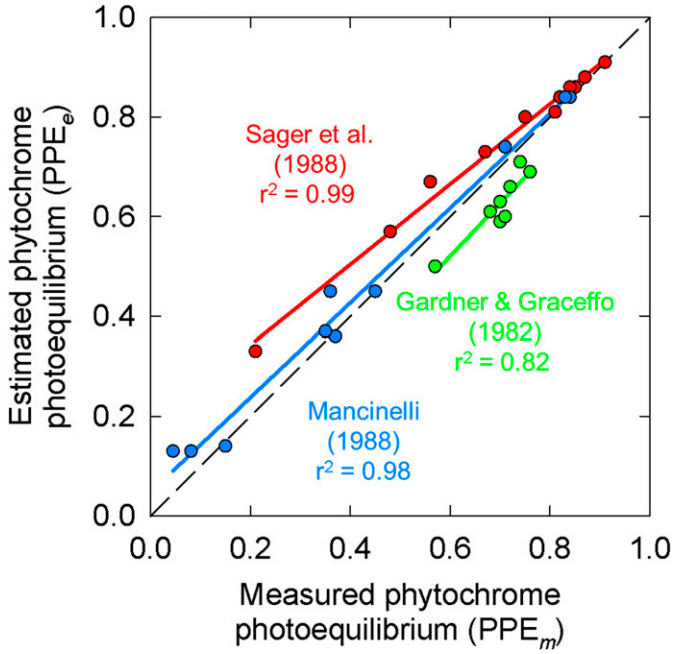

Fig. 1. Comparison of measured and estimated phytochrome photoequilibrium (PPE_m and PPE_e) from Gardner and Graceffo [1982 (green)], Sager et al. [1988 (red)], and Mancinelli [1988b (blue)].

1. ***Differences in weighting factors*** are discussed by Mancinelli (1986, 1988a). Up to the mid-1980s it was common to use weighting factors from Butler et al. (1964), but these weighting factors were obtained from less pure and more degraded phytochrome extractions compared with Kelly and Lagarias (1985), Lagarias et al. (1987), Sager et al. (1988), and Vierstra and Quail (1983a, 1983b). Beyond suggesting using newer vs. older data, Mancinelli (1986, 1988a) was unable to recommend a superior set of weighting factors, and only mentioned that the choice should be open to revision.

The weighting factors from these studies can have substantial differences on an absolute scale, and there are further differences when using weighting factors determined in vitro vs. in vivo (Gardner and Graceffo, 1982; Pratt and Briggs, 1966; Seyfriend and Schäfer, 1985), where in vivo data shows a marked decrease in the response to blue and ultraviolet photons. Rajapakse and Kelly (1994) demonstrated some of the potential differences in PPE_e under a single light source, and furthermore PPE_e and PPE_m do not perfectly match (Fig. 1). Fortunately, the most commonly used weighting factors from Kelly and Lagarias (1985), Lagarias et al. (1987), and Sager et al. (1988) are similar on a normalized scale. Despite this similarity, weighting factors primarily come from the monocots oat (*Avena sativa*) and rye (*Secale cereale*), which differ on an absolute scale (Lagarias et al., 1987), and their universal utility is uncertain.

2. ***Multiple phytochromes*** are present in dark-grown and etiolated tissue, but only phytochrome-B (phyB) appears to be primarily responsible for altering plant morphology in response to shade in adult, light grown plants. This conclusion is primarily because only monogenic mutants of *Arabidopsis thaliana* without phyB appear to have severe shade-avoidance symptoms in white light (Aukerman et al., 1997; Devlin et al., 1998, 1999; Franklin et al., 2003), whereas phyA- (Franklin and Quail, 2010; Whitelam et al., 1993), phyC- (Franklin et al., 2003), phyD- (Aukerman et al., 1997; Devlin et al., 1999), and phyE-deficient (Devlin et al., 1998) mutants appear indistinguishable from the wild type in the same conditions. The supporting role of these other phytochromes emerge in a phyB-deficient background (Aukerman et al., 1997; Devlin et al., 1998, 1999; Franklin et al., 2003), in which cases the double mutant shows more pronounced shade-avoidance symptoms in white light compared with the phyB-deficient monogenic mutant.

   In etiolated *Arabidopsis*, the percentages of the different pools of phytochrome protein are 85% phyA, 10% phyB, and 5% other (phyC, phyD, and phyE), but on transition into the light the total pool of phytochrome drops by 23-fold and the ratios are readjusted to 5% phyA, 40% phyB, and 55% other (Sharrock and Clack, 2002). Both PPE_m and PPE_e use dark-grown etiolated tissue, meaning that P_{fr}/P_{total} is based on an average mix of all the phytochromes, but primarily phyA. This may create issues when using PPE_m or PPE_e to estimate the state of phyB in response to shade. Some limited evidence suggests that the photochemical properties of phyA and phyB are similar (Ruddat et al., 1997), but they differ from the photochemical properties of phyC and phyE (Eichenberg et al., 2000).

3. ***Nonphotochemical reversions*** of P_{fr} to P_r are independent of light intensity and duration, but dependent on temperature (Jung et al., 2016; Legris et al., 2016). This thermal relaxation of the phytochrome molecule occurs both in the dark and in the light. This leads to a potential lower value for P_{fr}/P_{total} at warmer temperatures under a single SPD. This effect is increased at lower light intensities where the rates of photoconversion are slower (Sellaro et al., 2019). In addition, nuclear body formation and dimerization of phytochrome may alter the thermal stability of P_{fr} (Klose et al., 2015; Rausenberger et al., 2010).

4. ***Intermediates*** between P_r and P_{fr}, and between P_{fr} and P_r have been studied with flash photolysis, low-temperature spectroscopy, dehydration studies, and kinetics of absorbance changes (Kendrick and Spruit, 1977). The conversions between P_r and P_{fr} are not instantaneous processes. Instead, the conversions involve a number of short-lived intermediate forms. When transferred into the dark, P_{fr} (measured by a technique similar to that described in Supplemental Material 1) immediately increases to a level higher than the equilibrium level established in the light. This increase above photoequilibrium indicates that there is a rate-limiting chemical conversion between P_r and P_{fr}, leading to an accumulation of an intermediate under high light intensities. Kendrick et al. (1985) suggest that more than 50% of total phytochrome may be in intermediate forms in sunlight. Smith and Fork (1992) found similar results, indicating that the concentration of P_{fr} would decrease at high light intensities even if P_{fr}/P_{total} remained the same. Smith (1990) saw no long-term change in stem-extension rate at constant R:FR ratios under rapidly increasing or decreasing intensities, an effect that should have decreased or increased, respectively, the total concentration of P_{fr}. This is one of several experiments conducted by H. Smith that attempted to show that P_{fr}/P_{total} could predict responses better than the total amount of P_{fr}, suggesting that both P_{fr} and P_r may be active (Smith, 1981, 1982, 1983, 1990, 1994, 1995). His analysis was largely ignored in the literature, although Schmidt and Mohr (1982) suggested that P_{fr} was the better indicator.

5. ***P_{total} is not constant, as plant physiology textbooks often imply.*** Smith (1981) measured P_{total} in adult *Zea mays* tissue bleached with norflurazon and showed that P_{total} could change depending on the background SPD. Similarly, Schäfer (1978) showed that the synthesis and degradation rates of P_{total} in *Cucubita pepo* could change with plant age, and suggested that these rates may be under circadian control. The messenger RNA expression of phyB appears to be under circadian control (Kozma-Bognár et al., 1999; Tóth et al., 2001), and immunoblot analysis of total phyB protein concentrations have shown that it can change by 50% over the course of a day (Kozma-Bognár et al., 1999; Sharrock and Clack, 2002). This 50% variation in phyB protein indicates that although PPE_e provides an estimate of P_{fr} to P_{total}, the actual concentration of P_{fr} could fluctuate by 50%. Some of the other phytochromes (e.g., phyA) have shown an even more dramatic fluctuation over the course of the day. In addition, activated phyB interacts with the transcriptional factors phytochrome interacting factors (PIFs) resulting in their mutual ubiquitination followed by proteasomal degradation (Ni et al., 2014). This means that the rate of degradation depends on the concentration of PIFs. Further, the concentration of phyB is not as light stable as is commonly thought (Klose et al., 2015). Overall, these findings indicate that the total pool of phytochrome at a given point in the day can vary based on the circadian rhythm, the expression of PIFs, and the length of time in the dark or the light.

   Recent complex modeling approaches in *Arabidopsis* (Klose et al., 2015; Sellaro et al., 2019) have estimated the pool of active phyB (P_{fr}-P_{fr} homodimer) in the nucleus by including not only photoconversions, but also thermal reversions (mentioned previously) and synthesis/degradation rates. This model includes specific degradation rates for each of the three potential states of the dimer. The rates of synthesis are assumed to be constant, although this is likely not the case. Finally, there is no certainty as to how predictive this more complex model is for species other than *Arabidopsis*.

6. ***Chlorophyll*** in leaves attenuates the photon flux at different wavelengths. Therefore, P_{fr}/P_{total} (PPE_m or PPE_e) only represent the ratio at the top epidermal layer of leaves (Gardner and Graceffo, 1982; Morgan and Smith, 1978). However, even this may not be true, as back scattering and reflectance of photons may actually make the photon intensity in the initial layer of a leaf higher than that just above the leaf (Mancinelli, 1988a; Seyfried and Fukshansky, 1983). Morgan and Smith (1978) demonstrated that the correlation between log-stem-extension rate and PPE_e deviated from linearity when measured under a leaf with high chlorophyll content. Action spectra studies have shown that the peak wavelength of phytochrome responses in green tissue shift to shorter wavelengths than expected (Jose and Schäfer, 1978; Kasperbauer et al., 1963), indicating that some photon attenuation is occurring.

These six considerations bring the mechanistic relationship between P_{fr}/P_{total} and morphology into question. Early studies that compared PPE_m with growth responses used the technique described in Supplemental Material 1. This technique could

measure only the P_{fr}/P_{total} ratio and does not indicate concentrations of either P_{total} or P_{fr} (but see Supplemental Material 1). Because measurements and estimations of P_{fr}/P_{total} have predicted morphological responses, they were widely used as the primary metric, but due to the considerations discussed previously, what do PPE_m and PPE_e actually indicate?

As mentioned previously, studies have used a constant background spectrum and only adjusted amounts of R and FR (Kalaitzoglou et al., 2019; Morgan and Smith, 1976, 1978, 1979; Park and Runkle, 2017, 2018), meaning that the responses are equally well predicted by environmental factors like the R:FR ratio.

R and FR Photons as Environmental Signals

These challenges of mechanistically modeling phytochrome protein dynamics and linking them with morphological responses across a wide range of species and environments mean that simple environmental signals may be more broadly applicable. Small factors in complex biological models can have large impacts on outputs, especially when downstream processes remain unknown.

Environmental signals like temperature are easily measurable. Smith (1982) eloquently described the importance of environmental signals: *"For an environmental signal to be valuable to a perceiving organism it must be: a) unambiguous, b) reliable, c) readily detectable, and d) related to an ecologically important condition in some quantitatively predictive manner."*

Smith (1982) went on to state that the R:FR ratio perfectly fit these criteria as an environmental signal of vegetative shade, as other environmental photobiological signals of shade, like photon intensity, do not meet the same standard of reliability. Many authors investigating phytochrome action with mutant *Arabidopsis* avoid P_{fr}/P_{total} and simply use the R:FR ratio (de Wit et al., 2016; Trupkin et al., 2014; Wang et al., 2015).

Effect of Wavelength Range on the R:FR Ratio

Similar to the lack of standardization regarding weighting factors to calculate PPE_e, with some authors using data from Sager et al. (1988) and others using data from Kelly and Lagarias (1985), there is little standardization in the wavelength ranges for R and FR photon fluxes to calculate the R:FR ratio. This can result in different values of the R:FR ratio for a single light source that has a constant SPD. One of the earliest and most commonly used ranges was the integration of the photon flux between 655 and 665 nm divided by the photon flux between 725 and 735 nm. This range was widely used by H. Smith and colleagues (Holmes and Smith, 1977a, 1977b; Smith and Holmes, 1977). Smith, in correspondence with J. Monteith, settled on the Greek letter ζ (lower case zeta) to represent the ratio (Holmes and Smith, 1977a; Monteith, 1976). Smith reported that the R:FR ratio of sunlight following this method was 1.19 (Smith, 1982). He reported that there is surprisingly little variation in the R:FR ratio under a variety of environmental conditions (Smith, 1982), but that does not appear to be the case (Supplemental Material 2). A second method to calculate the R:FR ratio is to simply divide the photon flux at 660 nm by the flux at 730 nm (Deitzer et al., 1979; Pausch et al., 1991; Warrington et al., 1989). This single wavelength method for obtaining R and FR often uses alternative wavelengths like 645, 650, 725, and/or 735 nm (Casal et al., 1985; Kasperbauer, 1987; Kasperbauer and Karlen, 1994; Taylorson and Borthwick, 1969). M. Kasperbauer favored measuring R at 645 nm instead of 660 nm because of the apparent maximum sensitivity of floral inhibition by night break lighting at 645 nm (Kasperbauer et al., 1963) instead of the expected 660 nm (Butler et al., 1959). This shift in sensitivity when using green vs. etiolated tissue was speculated to be due to chlorophyll absorption. Jose and Schäfer (1978) found a similar shift in the action spectra for lengths of green vs. etiolated hypocotyls. Finally, a third approach has been to calculate the R:FR ratio based on the flux between 600 and 700 nm divided by the flux between 700 and 800 nm (Li and Kubota, 2009; Mortensen and Strømme, 1987; Rajapakse et al., 1992; Rajapakse and Kelly, 1994; Runkle and Heins, 2001). Figure 2 shows a comparison of four wavelength ranges using the ASTM G173-03 reference of global tilt solar energy flux [American Society for Testing and Materials, 2012 (converted to a photon flux)] and a measurement made at Utah State University (Logan, UT) at noon on 10 June 2020 using a spectroradiometer (PS-300; Apogee Instruments, Logan, UT). These three methods result in a 6% to 7% difference. These differences would be larger under narrow bandwidth LEDs. Although these are the most common methods used to calculate the R:FR ratio from spectral distribution measurements, there are numerous variations.

Sensors with dual detectors have been widely used to calculate an R:FR ratio. These sensors include photodiodes sensitive to photons in the R and FR regions. An early commercial model was the 660/730-nm sensor (SKR110;

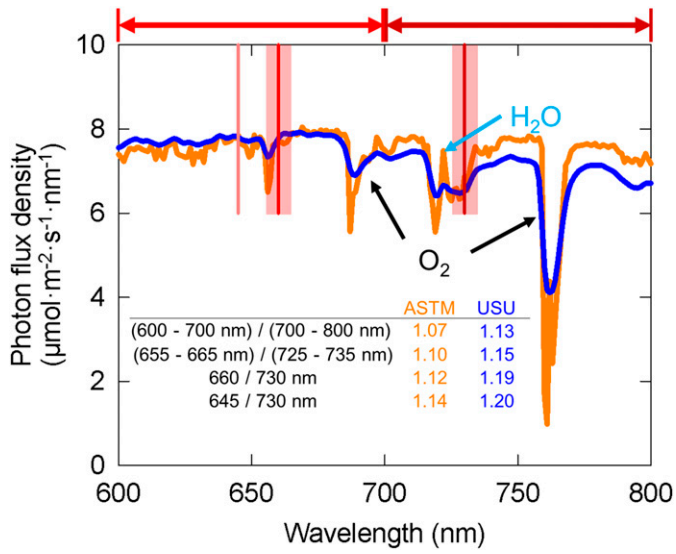

Fig. 2. Spectral photon distribution of the ASTM G173-03 reference of global tilt energy converted to photon flux [American Society for Testing and Materials, 2012 (orange line)] and a measurement made at Utah State University at noon on 10 June 2020 (blue line). Four ranges used for obtaining the red to far-red ratio (R:FR ratio) are shown as lines or bands in the figure: 1) 600 to 700 nm/700 to 800 nm shown as arrows at the top of the figure, 2) 655 to 665 nm/725 to 735 nm shown as shaded regions, 3) 660 / 730 nm shown as vertical lines, and 4) 645/730 nm shown as a separate vertical line. The corresponding calculation of the R:FR ratio is shown in inset table. This figure also demonstrates potential variation due to environmental conditions. The light blue arrow shows a water vapor absorbance band and the black arrows show an oxygen absorbance band.

Skye Instruments, Llandrindod Wells, UK), which used to be sensitive to photons from 630 to 665 for the R region, but this range was modified in 2010 to 645 to 675 nm. The FR range remained mostly unchanged from 715 to 740 nm, although it appears to have narrowed (Fig. 3). The Skye R:FR sensor was reported to provide a ratio of 1.1 in sunlight (Messier et al., 1989); we recently confirmed this measurement as 1.05. More recently, an R:FR sensor was developed with a wavelength range of 645 to 665 nm for R and 720 to 740 nm for FR (model S2, Apogee Instruments). R:FR sensors do not evenly weight the photons between these wavelengths (Fig. 3), but are less expensive, more portable, have a faster response time, and are more durable than spectroradiometers. Inexpensive spectroradiometers are now widely available, but these have lower spectral resolution (often greater than 24 nm bandwidth).

When calculating the R:FR ratio (and subsequent metrics described later in this article), we recommend that the most appropriate range for FR is 730 ± 10 nm. This is a larger range than the commonly used recommendation from H. Smith, but the variation in reported maximum absorbance of P_{fr} in the FR region justifies this wider range (Kelly and Lagarias, 1985; Sager et al., 1988; Seyfried and Schäfer, 1985). Broader ranges (e.g., 700 to 800 nm) could overestimate phytochrome responses from the sun or from LEDs that have peaks beyond 750 nm. The R range is more difficult to determine because of chlorophyll screening and the apparent shift in maximum sensitivity from ≈660 nm to ≈630 or 645 nm (Jose and Schäfer, 1978; Kasperbauer et al., 1963). Choice of either peak wavelength for R photons can be appropriate with justification. Similar to FR, a wider range (±10 nm) seems appropriate. Commercially available R:FR sensors use these wider ranges and are a good choice for quickly and affordably assessing incoming R and FR photons. When reporting spectral data in wider contexts than phytochrome responses, broader ranges still may be appropriate.

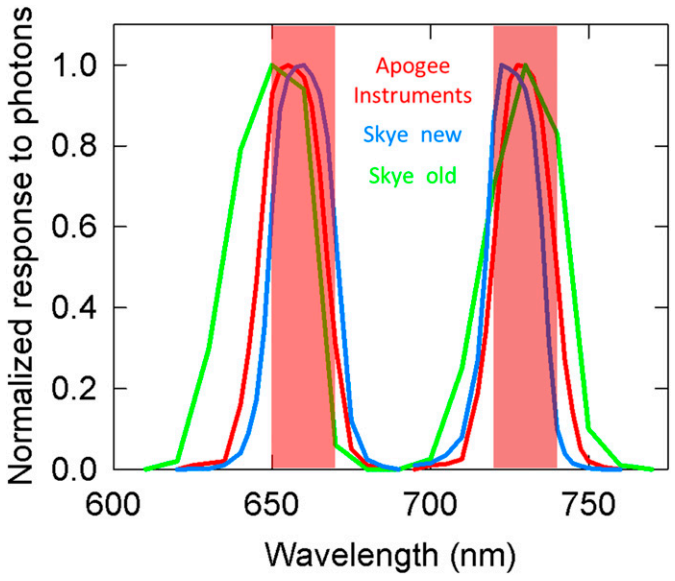

Fig. 3. Sensitivity of the red and far-red photodiodes in three red to far-red ratio sensors from Apogee instruments (Logan, UT) and Skye Instruments (Llandrindod Wells, UK).

Units to Measure the R:FR Ratio: Energy Flux vs. Photon Flux

Although some studies have used energy units to measure R and FR fluxes (Salisbury, 1981; Taylorson and Borthwick, 1969), most studies have used photon fluxes because photons were known to be the driving factor for phytochrome responses as far back as 1964 (Butler et al., 1964; Siegelman and Hendricks, 1964). This is also described by the Stark-Einstein Law/photochemical equivalence law (Roth, 2001). Photons at 660 nm are more energetic than photons at 730 nm, so an R:FR ratio (660/730 nm) in sunlight based on energy units is 1.24, whereas the ratio based on photon flux is 1.12. These measurements can be interconverted using Planck's equation ($micromoles\ of\ photons = Joules\ of\ energy \times \lambda(in\ nanometers) \times 0.008359$).

Effect of Environmental Conditions on R and FR Photon Flux

Atmospheric conditions also affect the R:FR ratio in natural environments. Kotilainen et al. (2020) demonstrated that atmospheric conditions, latitude, and time of day cause more variation in the R:FR ratio in the natural environment than previously thought. Photobiologists studying phytochrome responses in the natural environment need to be aware of this variation. We summarize these factors in Supplemental Material 2.

The Relationship between R:FR Ratio and PPE is Highly Nonlinear

The R:FR ratio has been an adequate metric for the natural environment because the highest value is ≈1.4 around midday (Kotilainen et al., 2020). Nonetheless, as measurements move from full sunlight to deep shade, the relative amount of FR increases and the R:FR ratio decreases. This confines the R:FR ratio in the natural environment to values ranging from ≈0 to 1.

Smith and Holmes (1977) plotted the relationship between R:FR ratio and PPE_m under sunlight, vegetative shade, and some electric lights. This analysis showed that PPE_m was highly sensitive to R:FR ratios found in shade. Smith (1982) recommends that this curve can be used to estimate P_{fr}/P_{total} from the R:FR ratio in natural environments, but he warns against using it in controlled environments, saying, *"the curve may be reliably used for all natural broadband sources except those, which contain a high portion of blue. Its use with artificial far-red sources is limited because of the difficulty of accurate read-out on the steepest part of the curve."*

Under electric lights, the flux of FR can approach zero and the R:FR ratio approaches infinity. Although P_{fr}/P_{total} may be unreliable, it does generally describe phytochrome status and it is useful to understand the relationships with the R:FR ratio. Figure 4A shows the relationship between R:FR ratio measured with a Skye R:FR sensor and PPE_e calculated from spectral measurements and weighting factors published by Sager et al. (1988). The relationship is highly nonlinear. Under LEDs with minimal FR, the R:FR ratio nearly flat-lines above 3, and values continue to slightly increase up to 1800. Some publications have reported R:FR ratios above 100 (Hernández and Kubota, 2016), whereas others have avoided the infinity problem by reporting the R:FR ratio as 1:0 (Park and Runkle, 2017, 2018). These issues mean that the R:FR ratio has little predictive value under electric lights.

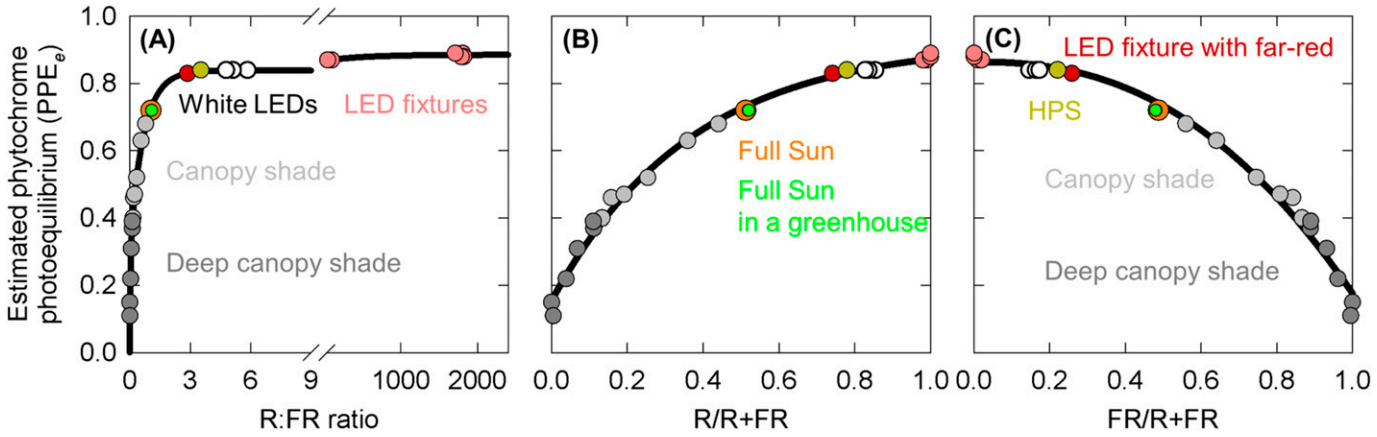

Fig. 4. (**A**) Relationship between red to far-red ratio (R:FR ratio), measured with a R:FR sensor (SKR110; Skye Instruments, Llandrindod Wells, UK) and estimated phytochrome photoequilibrum (PPE$_e$) using weighting factors from Sager et al. (1988). The R:FR ratio approaches infinity, but PPE reaches a maximum of 0.89. (**B**) Relationship between R fraction (R/R+FR) and estimated PPE. The curve is more linear. (**C**) Relationship between FR fraction and PPE$_e$. This ratio is positively correlated with growth parameters like stem length and leaf area, so this may be the preferred ratio. Both PPE$_e$ and R fraction are negatively correlated with stem length and leaf area.

R Fraction: An Intermediate Solution

A simple improvement is to use the red fraction (R fraction), first reported by Smith (1990), which is calculated as:

$$R\ fraction = \frac{R}{R+FR} = \frac{R:FR}{1+R:FR} \quad [1]$$

This confines the fraction (or ratio) to values between 0 and 1. We recommend the same ranges for R and FR as previously discussed for the R:FR ratio, but we note that confining the ratio from 0 to 1 can have a bigger impact than the wavelength range. We plot the same data as Fig. 4A by using the new R fraction instead of the R:FR ratio in Fig. 4B.

Smith (1990) showed that the relationship between the R fraction and the change in stem-extension rate in *Sinapis alba* was more linear than the relationship between PPE$_m$ and the change in stem-extension rate. But, the implications were not heavily discussed and the metric never became widely used.

P_{fr}/P_{total}, like the R fraction, is confined to values between 0 and 1. However, based on the photochemical properties, P_{fr}/P_{total} is actually confined to values between 0 and 0.89 (Lagarias et al., 1987, Fig. 4). R activates P_r into P_{fr} and FR reconverts P_{fr} back into P_r, so it makes sense that the R fraction (R/R+FR) is well correlated with PPE ($P_{fr} / P_r + P_{fr}$).

FR Fraction: An Improved Metric

The active form of phytochrome (P_{fr}) suppresses stem elongation by interacting with and degrading PIFs, which are involved in the expression of shade-avoidance (cell wall and auxin-related) genes (Casal, 2012; de Lucas and Prat, 2014). Therefore, P_{fr}/P_{total}, R fraction and the R:FR ratio have an inverse relationship with the parameters of interest in controlled environments like stem length (Morgan and Smith, 1976, 1978, 1979; Park and Runkle, 2017, 2018). Perhaps many researchers have used the R:FR ratio because in the natural environment it is generally confined to values between ≈0 and 1. An FR:R ratio would not be confined in the same way. But positive correlations are more intuitive than negative correlations, and thus the FR fraction is more intuitive than the R fraction. The FR fraction is the mirror image of the R fraction (Fig. 4C) and uses the same wavelength ranges described previously. It is calculated as follows:

$$FR\ fraction = \frac{FR}{R+FR} = \frac{1}{1+R:FR} \quad [2]$$

An FR:R ratio was used by M. Kasperbauer in several studies that investigated neighbor perception (Kasperbauer, 1971; Kasperbauer and Karlen, 1994) or reflectivity of colored mulches (Decoteau et al., 1990; Kasperbauer and Hunt, 1992). These studies do not provide an explanation for the use of the FR:R ratio, but the ratio is positively correlate with growth parameters.

Comparison of a Related Ratio that Evolved to Eventually Range from 0 to 1

The evolution to a simpler, more intuitive ratio has similarities with metrics used in remote sensing of vegetation. Jordan (1969) proposed the ratio vegetation index [RVI (reflectance at 900 nm divided by the reflectance at 680 nm)] to assess chlorophyll content and fraction of groundcover by leaves. But like the R:FR ratio, this original metric was nonlinear and approached infinity in dense vegetation. To reduce these issues, Tucker (1978) introduced the difference vegetation index (the difference in intensity between 900 and 680 nm), but this difference increased with light intensity, so it was later normalized to the intensity by dividing by the total photon flux. This resulted in a metric that ranges from 0 to 1 as the canopy density increases from bare soil to complete cover. This improved metric is now widely used and called the normalized difference vegetation index [NDVI (Gamon et al., 1995)].

Another metric that is still evolving is root mass fraction (root mass divided by total mass). Many researchers still publish root:shoot ratio (root mass divided by shoot mass), but this ratio starts at infinity in a germinating seed and decreases nonlinearly as the plant ages. By contrast, root mass

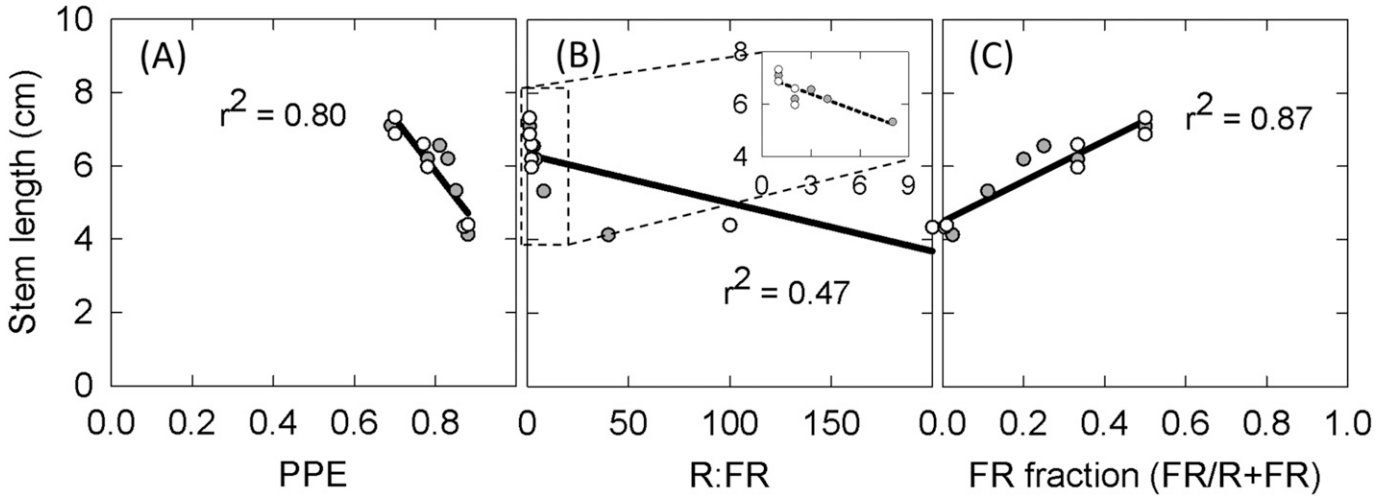

Fig. 5. Represented geranium ('Pinto Premium Orange Bicolor') stem length data estimated from two papers by Park and Runkle (2017, 2018). These data come from Fig. 2 in both papers. Gray circles are from the 2017 paper and were grown for 29 to 30 d. The open circles are from the 2018 paper and were grown for 36 to 39 d. Data are normalized to the grand mean of both studies. (**A**) The reported estimate of phytochrome photoequilibrium (PPE_e) compared with stem length. (**B**) The red to far-red ratio (R:FR ratio) compared with stem length. Because Park and Runkle report R:FR ratios with no FR as 1:0, we arbitrarily chose 0.005, 0.025, and 0.01 (relative to R = 1). Notice the extremely large scale of the x-axis and how the data are sensitive to the small value of FR that might be provided by a spectroradiometer. These values are not unreasonable, as they depend on the dark calibration and signal-to-noise ratio. (**C**) FR faction (FR/R+FR) compared with stem length. (**C**) uses the same data as (**B**) and are calculated using Eq. [2]. Notice that the FR fraction is not nearly as sensitive to small quantities of FR compared with the R:FR ratio.

fraction starts at 1 and slowly decreases over the life cycle. Metrics that use a total in the denominator are more intuitive.

A Comparison of Metrics

To demonstrate the value of this improved index, we normalize (to the grand mean of both studies) and regraph geranium (*Pelargonium* ×*hortorum* 'Pinto Premium Orange Bicolor') stem length data from Park and Runkle (2017, 2018) using PPE_e, the R:FR ratio, and the FR fraction as the independent variable (Fig. 5). It should be noted that the R:FR ratio and FR fraction are calculated with wider 100-nm bandwidths rather than the narrower 20-nm bandwidths we suggested earlier. This is because these authors reported R and FR in these 100-nm bands. In addition, because these data come from a study that uses LEDs centered at ≈660 and 730 nm (with no white LEDs), the 100-nm range and the 20-nm range would produce very similar results. We exclude data from the most recent publication by these authors because it also altered the amount of blue, inducing morphological effects outside the R and FR ranges (Park and Runkle, 2019). These data contain three R:FR ratios that do not have any FR, which the authors report as 1:0. Because division by zero is undefined, we arbitrarily set FR equal to 0.01, 0.025, and 0.05 (relative to R = 1) in these cases (Fig. 5B and C). The alternative is to assign these FR values the same low value, but this would have caused clumping of data, which may not occur in LED fixtures (see the flat part of Fig. 4A). In addition, the arbitrary values demonstrate the hyperbolic function often seen when graphing data with the R:FR ratio. Our arbitrary values can be obtained with a spectroradiometer, but the measurement depends on the dark calibration and signal-to-noise ratio.

Between 0 and 10, the R:FR ratio is still a good predictor of stem length (Fig. 5B, inset), but large R and small FR values significantly alter the correlation between the R:FR ratio and stem length (Fig. 5B) and the curve is highly nonlinear. Especially in sole-source LED plant factories, which often lack FR, the R:FR ratio is clearly a poor metric to predict phytochrome-controlled responses. Zhang et al. (2020) similarly concluded that the R:FR ratio could change drastically while PPE_e remained relatively constant. They further found that the growth in *Antirrhinum majus*, *Petunia* ×*hybrida*, and *Zinnia elegans* was better correlated with PPE_e than the R:FR ratio, indicating that this was the superior metric. PPE_e presented here also appears to be a reasonably good metric. However, as we have discussed previously, there are good reasons to be skeptical of this approach. As we learn more about phytochrome kinetics and downstream processes, this ratio may be incorporated into complex and mechanistic models that have better predictive ability, but for now perhaps environmental signals are better metrics.

The FR fraction (and the R fraction, not shown) is not sensitive to extremely high R or low FR (Fig. 5C). These examples demonstrate that the FR fraction is intuitively correlated with shade-avoidance growth parameters and confined to values from 0 to 1. This metric is well suited to controlled environment plant production. In addition, because experiments performed in controlled environments are used to predict responses in the natural environment, this may indicate that it is also a better metric under natural conditions.

It is important to remember that the R:FR ratio, PPE, and the FR fraction can only predict morphological responses caused by phytochrome. The effects of blue light are not assessed with these metrics. Although PPE_e includes some sensitivity to violet and ultraviolet photons, these effects are minimal compared with blue light receptors like cryptochromes (Park and Runkle, 2019; Runkle and Heins, 2001). Cryptochromes interact with many of the same transcription factors as phytochrome (de Wit et al., 2016). Blue and green photons have been proposed to act antagonistically in a

manner similar to R and FR (Banerjee et al., 2007; Bouly et al., 2007), and thus models describing cryptochrome kinetics have been developed that resemble phytochrome kinetic models (Procopio et al., 2016). Future studies should investigate interactions of the R and blue photons antagonistically acting against FR and green photons.

Literature Cited

American Society for Testing and Materials. 2012. Committee G03 on Weathering and Durability. Standard tables for reference solar spectral irradiances: Direct normal and hemispherical on 37° tilted surface. ASTM Int., West Conshohocken, PA.

Aukerman, M.J., M. Hirschfeld, L. Wester, M. Weaver, T. Clack, R.M. Amasino, and R.A. Sharrock. 1997. A deletion in the PHYD gene of the *Arabidopsis* Wassilewskija ecotype defines a role for phytochrome D in red/far-red light sensing. Plant Cell 9:1317–1326, doi: 10.1105/tpc.9.8.1317.

Banerjee, R., E. Schleicher, S. Meier, R.M. Viana, R. Pokorny, M. Ahmad, R. Bittl, and A. Batschauer. 2007. The signaling state of *Arabidopsis* cryptochrome 2 contains flavin semiquinone. J. Biol. Chem. 282:14916–14922, doi: 10.1074/jbc.M700616200.

Borthwick, H.A., S.B. Hendricks, M.W. Parker, E.H. Toole, and V.K. Toole. 1952. A reversible photoreaction controlling seed germination. Proc. Natl. Acad. Sci. USA 38:662–666, doi: 10.1073/pnas.38.8.662.

Bouly, J.P., E. Schleicher, M. Dionisio-Sese, F. Vandenbussche, D. Van Der Straeten, N. Bakrim, S. Meier, A. Batschauer, P. Galland, R. Bittl, and M. Ahmad. 2007. Cryptochrome blue light photoreceptors are activated through interconversion of flavin redox states. J. Biol. Chem. 282:9383–9391, doi: 10.1074/jbc.M609842200.

Butler, W.L., K.H. Norris, H.W. Siegelman, and S.B. Hendricks. 1959. Detection, assay, and preliminary purification of the pigment controlling photoresponsive development of plants. Proc. Natl. Acad. Sci. USA 45:1703–1708, doi: 10.1073/pnas.45.12.1703.

Butler, W.L., H.C. Lane, and H.W. Siegelman. 1963. Nonphotochemical transformations of phytochrome in vivo. Plant Physiol. 38:514–519, doi: 10.1104/pp.38.5.514.

Butler, W.L., S.B. Hendricks, and H.W. Siegelman. 1964. Action spectra of phytochrome *in vitro*. Photochem. Photobiol. 3:521–528, doi: 10.1111/j.1751-1097.1964.tb08171.x.

Casal, J.J., V.A. Deregibus, and R.A. Sanchez. 1985. Variations in tiller dynamics and morphology in *Lolium multiflorum* Lam. vegetative and reproductive plants as affected by differences in red/far-red irradiation. Ann. Bot. 56:553–559, doi: 10.1093/oxfordjournals.aob.a087040.

Casal, J.J. 2012. Shade avoidance. Arabidopsis Book 10:e0157, doi: 10.1199/tab.0157.

Chen, M. and J. Chory. 2011. Phytochrome signaling mechanisms and the control of plant development. Trends Cell Biol. 21:664–671, doi: 10.1016/j.tcb.2011.07.002.

Cumming, B.G. 1963. The dependence of germination on photoperiod, light quality, and temperature in *Chenopodium* spp. Can. J. Bot. 41:1211–1233, doi: 10.1139/b63-102.

de Lucas, M. and S. Prat. 2014. PIF s get BR right: PHYTOCHROME INTERACTING FACTOR s as integrators of light and hormonal signals. New Phytol. 202:1126–1141, doi: 10.1111/nph.12725.

de Wit, M., D.H. Keuskamp, F.J. Bongers, P. Hornitschek, C.M. Gommers, E. Reinen, C. Martínez-Cerón, C. Fankhauser, and R. Pierik. 2016. Integration of phytochrome and cryptochrome signals determines plant growth during competition for light. Curr. Biol. 26:3320–3326, doi: 10.1016/j.cub.2016.10.031.

Decoteau, D.R., M.J. Kasperbauer, and P.G. Hunt. 1990. Bell pepper plant development over mulches of diverse colors. HortScience 25:460–462, doi: 10.21273/HORTSCI.25.4.460.

Deitzer, G.F., R. Hayes, and M. Jabben. 1979. Kinetics and time dependence of the effect of far red light on the photoperiodic induction of flowering in Wintex barley. Plant Physiol. 64:1015–1021, doi: 10.1104/pp.64.6.1015.

Devlin, P.F., S.R. Patel, and G.C. Whitelam. 1998. Phytochrome E influences internode elongation and flowering time in *Arabidopsis*. Plant Cell 10:1479–1487, doi: 10.1105/tpc.10.9.1479.

Devlin, P.F., P.R. Robson, S.R. Patel, L. Goosey, R.A. Sharrock, and G.C. Whitelam. 1999. Phytochrome D acts in the shade-avoidance syndrome in *Arabidopsis* by controlling elongation growth and flowering time. Plant Physiol. 119:909–916, doi: 10.1104/pp.119.3.909.

Dooskin, R.H. and A.L. Mancinelli. 1968. Phytochrome decay and coleoptile elongation in *Avena* following various light treatments. Bul. Torrey Bot. Club 95:474–487, doi: 10.2307/2483479.

Eichenberg, K., I. Bäurle, N. Paulo, R.A. Sharrock, W. Rüdiger, and E. Schäfer. 2000. *Arabidopsis* phytochromes C and E have different spectral characteristics from those of phytochromes A and B. FEBS Lett. 470:107–112, doi: 10.1016/S0014-5793(00)01301-6.

Franklin, K.A., S.J. Davis, W.M. Stoddart, R.D. Vierstra, and G.C. Whitelam. 2003. Mutant analyses define multiple roles for phytochrome C in *Arabidopsis* photomorphogenesis. Plant Cell 15:1981–1989, doi: 10.1105/tpc.015164.

Franklin, K.A. and G.C. Whitelam. 2005. Phytochromes and shade-avoidance responses in plants. Ann. Bot. 96:169–175, doi: 10.1093/aob/mci165.

Franklin, K.A. and P.H. Quail. 2010. Phytochrome functions in *Arabidopsis* development. J. Expt. Bot. 61:11–24, doi: 10.1093/jxb/erp304.

Gamon, J.A., C.B. Field, M.L. Goulden, K.L. Griffin, A.E. Hartley, G. Joel, J. Peñuelas, and R. Valentini. 1995. Relationships between NDVI, canopy structure, and photosynthesis in three Californian vegetation types. Ecol. Appl. 5:28–41, doi: 10.2307/1942049.

Gardner, G. and M.A. Graceffo. 1982. The use of a computerized spectroradiometer to predict phytochrome photoequilibria under polychromatic irradiation. Photochem. Photobiol. 36:349–354, doi: 10.1111/j.1751-1097.1982.tb04385.x.

Hartmann, K.M. 1966. A general hypothesis to interpret 'high energy phenomena' of photomorphogenesis on the basis of phytochrome. Photochem. Photobiol. 5:349–365, doi: 10.1111/j.1751-1097.1966.tb05937.x.

Hendricks, S.B. and H.A. Borthwick. 1963. Control of plant growth by light, p. 233–262. In: L.T. Evans (ed.). Environmental control of plant growth. Academic Press, Cambridge, MA. doi: 10.1016/B978-0-12-244350-3.50018-5.

Hernández, R. and C. Kubota. 2016. Physiological responses of cucumber seedlings under different blue and red photon flux ratios using LEDs. Environ. Expt. Bot. 12:66–74, doi: 10.1016/j.envexpbot.2015.04.001.

Holmes, M.G. and H. Smith. 1975. The function of phytochrome in plants growing in the natural environment. Nature 254:512–514, doi: 10.1038/254512a0.

Holmes, M.G. and H. Smith. 1977a. The function of phytochrome in the natural environment—I. Characterization of daylight for studies in photomorphogenesis and photoperiodism. Photochem. Photobiol. 25:533–538, doi: 10.1111/j.1751-1097.1977.tb09124.x.

Holmes, M.G. and H. Smith. 1977b. The function of phytochrome in the natural environment—II. The influence of vegetation canopies on the spectral energy distribution of natural daylight. Photochem. Photobiol. 25:539–545, doi: 10.1111/j.1751-1097.1977.tb09125.x.

Johnson, R.E., Y. Kong, and Y. Zheng. 2020. Elongation growth mediated by blue light varies with light intensities and plant species: A comparison with red light in arugula and mustard seedlings. Environ. Expt. Bot. 169:103898, doi: 10.1016/j.envexpbot.2019.103898.

Jordan, C.F. 1969. Derivation of leaf-area index from quality of light on the forest floor. Ecology 50:663–666, doi: 10.2307/1936256.

Jose, A.M. and E. Schäfer. 1978. Distorted phytochrome action spectra in green plants. Planta 138:25–28, doi: 10.1007/BF00392909.

Jung, J.H., M. Domijan, C. Klose, S. Biswas, D. Ezer, M. Gao, A.K. Khattak, M.S. Box, V. Charoensawan, S. Cortijo, M. Kumar, A. Grant, J.C.W. Locke, E. Schäfer, K.E. Jaeger, and P.A. Wigge. 2016. Phytochromes function as thermosensors in *Arabidopsis*. Science 354:886–889, doi: 10.1126/science.aaf6005.

Kalaitzoglou, P., W. van Ierpen, J. Harbinson, M. van der Meer, S. Martinakos, K. Weerheim, C.C.S. Nicole, and L.F.M. Marcelis. 2019. Effects of continuous or end-of-day far-red light on tomato plant growth, morphology, light absorption, and fruit production. Front. Plant Sci. 10:322, doi: 10.3389/fpls.2019.00322.

Kasperbauer, M.J., H.A. Borthwick, and S.B. Hendricks. 1963. Inhibition of flowering of *Chenopodium rubrum* by prolonged far-red radiation. Bot. Gaz. 124:444–451, doi: 10.1086/336234.

Kasperbauer, M.J. 1971. Spectral distribution of light in a tobacco canopy and effects of end-of-day light quality on growth and development. Plant Physiol. 47:775–778, doi: 10.1104/pp.47.6.775.

Kasperbauer, M.J. 1987. Far-red light reflection from green leaves and effects on phytochrome-mediated assimilate partitioning under field conditions. Plant Physiol. 85:350–354, doi: 10.1104/pp.85.2.350.

Kasperbauer, M.J. and P.G. Hunt. 1992. Cotton seedling morphogenic responses to FR/R ratio reflected from different colored soils and soil covers. Photochem. Photobiol. 56:579–584, doi: 10.1111/j.1751-1097.1992.tb02205.x.

Kasperbauer, M.J. and D.L. Karlen. 1994. Plant spacing and reflected far-red light effects on phytochrome-regulated photosynthate allocation in corn seedlings. Crop Sci. 34:1564–1569, doi: 10.2135/cropsci1994.0011183X003400060027x.

Kelly, J.M. and J.C. Lagarias. 1985. Photochemistry of 124-kilodalton *Avena* phytochrome under constant illumination in vitro. Biochemistry 24:6003–6010, doi: 10.1021/bi00342a047.

Kendrick, R.E. and B. Frankland. 1968. Kinetics of phytochrome decay in *Amaranthus* seedlings. Planta 82:317–320, doi: 10.1007/BF00386434.

Kendrick, R.E. and C.J.P. Spruit. 1977. Phototransformations of phytochrome. Photochem. Photobiol. 26:201–214, doi: 10.1111/j.1751-1097.1977.tb07473.x.

Kendrick, R.E., J. Kome, and P.A.P.M. Jaspers. 1985. Kinetics of Pfr appearance in *Amaranthus caudatus*. Photochem. Photobiol. 42:785–787, doi: 10.1111/j.1751-1097.1985.tb01648.x.

Kilsby, C.A.H. and C.B. Johnson. 1982. The *in vivo* spectrophotometric assay of phytochrome in two mature dicotyledonous plants. Photochem. Photobiol. 35:255–260, doi: 10.1111/j.1751-1097.1982.tb03843.x.

Kim, H.J., M.Y. Lin, and C.A. Mitchell. 2019. Light spectral and thermal properties govern biomass allocation in tomato through morphological and physiological changes. Environ. Expt. Bot. 157:228–240, doi: 10.1016/j.envexpbot.2018.10.019.

Klein, W.H., J.L. Edwards, and W. Shropshire. 1967. Spectrophotometric measurements of phytochrome in vivo and their correlation with photomorphogenic responses of *Phaseolus*. Plant Physiol. 42:264–270, doi: 10.1104/pp.42.2.264.

Klose, C., F. Venezia, A. Hussong, S. Kircher, E. Schäfer, and C. Fleck. 2015. Systematic analysis of how phytochrome B dimerization determines its specificity. Nat. Plants 1:1–9, doi: 10.1038/nplants.2015.90.

Klose, C. 2019. vivo spectroscopy, p. 113–120. In: A. Hiltbrunner (ed.). Phytochromes. Humana Press, New York, NY. doi: 10.1007/978-1-4939-9612-4_8.

Kotilainen, T., P.J. Aphalo, C.C. Brelsford, H. Böök, S. Devraj, A. Heikkilä, R. Hernández, A. Kylling, A.V. Lindfors, and T.M. Robson. 2020. Patterns in the spectral composition of sunlight and biologically meaningful spectral photon ratios as affected by atmospheric factors. Agr. For. Meteorol. 291:108041, doi: 10.1016/j.agrformet.2020.108041.

Kozma-Bognár, L.K., A. Hall, É. Adám, S.C. Thain, F. Nagy, and A.J. Millar. 1999. The circadian clock controls the expression pattern of the circadian input photoreceptor, phytochrome B. Proc. Natl. Acad. Sci. USA 96:14652–14657, doi: 10.1073/pnas.96.25.14652.

Kusuma, P., P.M. Pattison, and B. Bugbee. 2020. From physics to fixtures to food: Current and potential LED efficacy. Hort. Res. 7:1–9, doi: 10.1038/s41438-020-0283-7.

Lagarias, J.C., J.M. Kelly, K.L. Cyr, and W.O. Smith, Jr. 1987. Comparative photochemical analysis of highly purified 124 kilodalton oat and rye phytochromes *in vitro*. Photochem. Photobiol. 46:5–13, doi: 10.1111/j.1751-1097.1987.tb04729.x.

Lamparter, T., J. Hughes, and E. Hartmann. 1994. A fully automated dual-wavelength photometer for phytochrome measurements and its application to phytochrome from chlorophyll containing extrace. Photochem. Photobiol. 60:179–183, doi: 10.1111/j.1751-1097.1994.tb05088.x.

Legris, M., C. Klose, E.S. Burgie, C.C. Rojas, M. Neme, A. Hiltbrunner, P.A. Wigge, E. Schäfer, R.D. Vierstra, and J.J. Casal. 2016. Phytochrome B integrates light and temperature signals in *Arabidopsis*. Science 354:897–900, doi: 10.1126/science.aaf5656.

Legris, M., Y.Ç. Ince, and C. Fankhauser. 2019. Molecular mechanisms underlying phytochrome-controlled morphogenesis in plants. Nat. Commun. 10:1–15, doi: 10.1038/s41467-019-13045-0.

Li, Q. and C. Kubota. 2009. Effects of supplemental light quality on growth and phytochemicals of baby leaf lettuce. Environ. Expt. Bot. 67:59–64, doi: 10.1016/j.envexpbot.2009.06.011.

Mancinelli, A.L. 1986. Comparison of spectral properties of phytochromes from different preparations. Plant Physiol. 82:956–961, doi: 10.1104/pp.82.4.956.

Mancinelli, A.L. 1988a. Some thoughts about the use of predicted values of the state of phytochrome in plant photomorphogenesis research. Plant Cell Environ. 11:429–439, doi: 10.1111/j.1365-3040.1988.tb01780.x.

Mancinelli, A.L. 1988b. Phytochrome photoconversion *in vivo*: Comparison between measured and predicted rates. Plant Physiol. 86:749–753, doi: 10.1104/pp.86.3.749.

Mancinelli, A.L. 1994. The physiology of phytochrome action, p. 221–269. In: R.E. Kendrick and G.H.M. Kronenberg (eds.). Photomorphogenesis in plants. Springer, Dordrecht, The Netherlands. doi: 10.1007/978-94-011-1884-2_10.

Meng, Q., N. Kelly, and E.S. Runkle. 2019. Substituting green or far-red radiation for blue radiation induces shade avoidance and promotes growth in lettuce and kale. Environ. Expt. Bot. 162:383–391, doi: 10.1016/j.envexpbot.2019.03.016.

Messier, C., T.W. Honer, and J.P. Kimmins. 1989. Photosynthetic photon flux density, red:far-red ratio, and minimum light requirement for survival of *Gaultheria shallon* in western red cedar–western hemlock stands in coastal British Columbia. Can. J. For. Res. 19:1470–1477, doi: 10.1139/x89-223.

Monteith, J.L. 1976. Spectral distribution of light in leaves and foliage, p. 447–460. In: H. Smith (ed.). Light and plant development. Butterworth, London, UK. doi: 10.1016/B978-0-408-70719-0.50032-2.

Morgan, D.C. and H. Smith. 1976. Linear relationship between phytochrome photoequilibrium and growth in plants under simulated natural radiation. Nature 262:210–212, doi: 10.1038/262210a0.

Morgan, D.C. and H. Smith. 1978. The relationship between phytochrome-photoequilibrium and development in light grown *Chenopodium album* L. Planta 142:187–193, doi: 10.1007/BF00388211.

Morgan, D.C. and H. Smith. 1979. A systematic relationship between phytochrome-controlled development and species habitat, for plants grown in simulated natural radiation. Planta 145:253–258, doi: 10.1007/BF00454449.

Mortensen, L.M. and E. Strømme. 1987. Effects of light quality on some greenhouse crops. Scientia Hort. 33:27–36, doi: 10.1016/0304-4238(87)90029-X.

Ni, W., S.L. Xu, J.M. Tepperman, D.J. Stanley, D.A. Maltby, J.D. Gross, A.L. Burlingame, Z.Y. Wang, and P.H. Quail. 2014. A mutually assured destruction mechanism attenuates light signaling

in *Arabidopsis*. Science 344:1160–1164, doi: 10.1126/science.1250778.
Park, Y. and E.S. Runkle. 2017. Far-red radiation promotes growth of seedlings by increasing leaf expansion and whole-plant net assimilation. Environ. Expt. Bot. 136:41–49, doi: 10.1016/j.envexpbot.2016.12.013.
Park, Y. and E.S. Runkle. 2018. Far-red radiation and photosynthetic photon flux density independently regulate seedling growth but interactively regulate flowering. Environ. Expt. Bot. 155:206–216, doi: 10.1016/j.envexpbot.2018.06.033.
Park, Y. and E.S. Runkle. 2019. Blue radiation attenuates the effects of the red to far-red ratio on extension growth but not on flowering. Environ. Expt. Bot. 168:103871, doi: 10.1016/j.envexpbot.2019.103871.
Pausch, R.C., S.J. Britz, and C.L. Mulchi. 1991. Growth and photosynthesis of soybean (*Glycine max* L. Merr.) in simulated vegetation shade: Influence of the ratio of red to far-red radiation. Plant Cell Environ. 14:647–656, doi: 10.1111/j.1365-3040.1991.tb01537.x.
Patadia, F., R.C. Levy, and S. Mattoo. 2018. Correcting for trace gas absorption when retrieving aerosol optical depth from satellite observations of reflected shortwave radiation. Atmos. Meas. Tech. 11:3205–3219, doi: 10.5194/amt-11-3205-2018.
Poel, B.R. and E.S. Runkle. 2017. Spectral effects of supplemental greenhouse radiation on growth and flowering of annual bedding plants and vegetable transplants. HortScience 52:1221–1228, doi: 10.21273/HORTSCI12135-17.
Pratt, L.H. and W.R. Briggs. 1966. Photochemical and nonphotochemical reactions of phytochrome in vivo. Plant Physiol. 41:467–474, doi: 10.1104/pp.41.3.467.
Pratt, L.H. 1975. Photochemistry of high molecular weight phytochrome *in vitro*. Photochem. Photobiol. 22:33–36, doi: 10.1111/j.1751-1097.1975.tb06717.x.
Procopio, M., J. Link, D. Engle, J. Witczak, T. Ritz, and M. Ahmad. 2016. Kinetic modeling of the *Arabidopsis* cryptochrome photocycle: FADHo accumulation correlates with biological activity. Front. Plant Sci. 7:888, doi: 10.3389/fpls.2016.00888.
Rajapakse, N.C., R.K. Pollock, M.J. McMahon, J.W. Kelly, and R.E. Young. 1992. Interpretation of light quality measurements and plant response in spectral filter research. HortScience 27:1208–1211, doi: 10.21273/HORTSCI.27.11.1208.
Rajapakse, N.C. and J.W. Kelly. 1994. Problems of reporting spectral quality and interpreting phytochrome-mediated responses. HortScience 29:1404–1407, doi: 10.21273/HORTSCI.29.12.1404.
Rausenberger, J., A. Hussong, S. Kircher, D. Kirchenbauer, J. Timmer, F. Nagy, E. Schäfer, and C. Fleck. 2010. An integrative model for phytochrome B mediated photomorphogenesis: From protein dynamics to physiology. PLoS One 5:e10721, doi: 10.1371/journal.pone.0010721.
Roth, H.D. 2001. Twentieth century developments in photochemistry. Brief historical sketches. Pure Appl. Chem. 73:395–403.
Runkle, E.S. and R.D. Heins. 2001. Specific functions of red, far red, and blue light in flowering and stem extension of long-day plants. J. Amer. Soc. Hort. Sci. 126:275–282, doi: 10.21273/JASHS.126.3.275.
Ruddat, A., P. Schmidt, C. Gatz, S.E. Braslavsky, W. Gärtner, and K. Schaffner. 1997. Recombinant type A and B phytochromes from potato. Transient absorption spectroscopy. Biochemistry 36:103–111, doi: 10.1021/bi962012w.
Sager, J.C., W.O. Smith, Jr., J.L. Edwards, and K.L. Cyr. 1988. Photosynthetic efficiency and phytochrome photoequilibria determination using spectral data. Trans. ASAE 31:1882–1889, doi: 10.13031/2013.30952.
Salisbury, F.B. 1981. Twilight effect: Initiating dark measurement in photoperiodism of *Xanthium*. Plant Physiol. 67:1230–1238, doi: 10.1104/pp.67.6.1230.
Schäfer, E. 1978. Variation in the rates of synthesis and degradation of phytochrome in cotyledons of *Cucurbita pepo* L. during seedling development. Photochem. Photobiol. 27:775–780, doi: 10.1111/j.1751-1097.1978.tb07676.x.
Schmidt, R. and H. Mohr. 1982. Evidence that a mustard seedling responds to the amount of P_{fr} and not to the P_{fr}/P_{tot} ratio. Plant Cell Environ. 5:495–499, doi: 10.1111/1365-3040.ep11611856.
Sellaro, R., R.W. Smith, M. Legris, C. Fleck, and J.J. Casal. 2019. Phytochrome B dynamics departs from photoequilibrium in the field. Plant Cell Environ. 42:606–617, doi: 10.1111/pce.13445.
Seyfried, M. and L. Fukshansky. 1983. Light gradients in plant tissue. Appl. Opt. 22:1402–1408, doi: 10.1364/AO.22.001402.
Seyfried, M. and E. Schäfer. 1985. Action spectra of phytochrome *in vivo*. Photochem. Photobiol. 42:319–326, doi: 10.1111/j.1751-1097.1985.tb08947.x.
Sharrock, R.A. and T. Clack. 2002. Patterns of expression and normalized levels of the five *Arabidopsis* phytochromes. Plant Physiol. 130:442–456, doi: 10.1104/pp.005389.
Siegelman, H.W. and S.B. Hendricks. 1964. Phytochrome and its control of plant growth and development. Adv. Enzymol. Relat. Areas Mol. Biol. 26:1–33, doi: 10.1002/9780470122716.ch1.
Smith, H. 1973. Light quality and germination: Ecological implications, p. 219–231. In: W. Heydecker (ed.). Seed ecology. Pennsylvania State Univ. Press, University Park, PA.
Smith, H. and M.G. Holmes. 1977. The function of phytochrome in the natural environment—III. Measurement and calculation of phytochrome photoequilibria. Photochem. Photobiol. 25:547–550, doi: 10.1111/j.1751-1097.1977.tb09126.x.
Smith, H. 1981. Evidence that P_{fr} is not the active form of phytochrome in light-grown maize. Nature 293:163–165, doi: 10.1038/293163a0.
Smith, H. 1982. Light quality, photoperception, and plant strategy. Annu. Rev. Plant Physiol. 33:481–518, doi: 10.1146/annurev.pp.33.060182.002405.
Smith, H. 1983. Is P_{fr} the active form of phytochrome? Philos. Trans. R. Soc. Lond. 303:443–452, doi: 10.1098/rstb.1983.0105.
Smith, H. 1990. Phytochrome action at high photon fluence rates: Rapid extension rate responses of light-grown mustard to variations in fluence rate and red:far-red ratio. Photochem. Photobiol. 52:131–142, doi: 10.1111/j.1751-1097.1990.tb01766.x.
Smith, H. and D.C. Fork. 1992. Direct measurement of phytochrome photoconversion intermediates at high photon fluence rates. Photochem. Photobiol. 56:599–606, doi: 10.1111/j.1751-1097.1992.tb02208.x.
Smith, H. 1994. Sensing the light environment: The functions of the phytochrome family, p. 377–416. In: R.E. Kendrick and G.H.M. Kronenberg (eds.). Photomorphogenesis in plants. Springer, Dordrecht, The Netherlands. doi: 10.1007/978-94-011-1884-2_15.
Smith, H. 1995. Physiological and ecological function within the phytochrome family. Annu. Rev. Plant Biol. 46:289–315, doi: 10.1146/annurev.pp.46.060195.001445.
Taylorson, R.B. and H.A. Borthwick. 1969. Light filtration by foliar canopies: Significance for light-controlled weed seed germination. Weed Sci. 17:48–51, doi: 10.1017/S0043174500030873.
Tóth, R., E. Kevei, A. Hall, A.J. Millar, F. Nagy, and L. Kozma-Bognár. 2001. Circadian clock-regulated expression of phytochrome and cryptochrome genes in *Arabidopsis*. Plant Physiol. 127:1607–1616, doi: 10.1104/pp.010467.
Trupkin, S.A., M. Legris, A.S. Buchovsky, M.B.T. Rivero, and J.J. Casal. 2014. Phytochrome B nuclear bodies respond to the low red to far-red ratio and to the reduced irradiance of canopy shade in *Arabidopsis*. Plant Physiol. 165:1698–1708, doi: 10.1104/pp.114.242438.
Tucker, C.J. 1978. Red and photographic infrared linear combinations for monitoring vegetation. Remote Sens. Environ. 8:127–150, doi: 10.1016/0034-4257(79)90013-0.
Vierstra, R.D. and P.H. Quail. 1983a. Photochemistry of 124 kilodalton *Avena* phytochrome *in vitro*. Plant Physiol. 72:264–267, doi: 10.1104/pp.72.1.264.
Vierstra, R.D. and P.H. Quail. 1983b. Purification and initial characterization of 124 kdalton phytochrome from *Avena*. Biochemistry 22:2498–2505, doi: 10.1021/bi00279a029.

Wang, Y., T. Zhang, and K.M. Folta. 2015. Green light augments far-red-light-induced shade response. Plant Growth Regulat. 77:147–155, doi: 10.1007/s10725-015-0046-x.

Warrington, I.J., D.A. Rook, D.C. Morgan, and H.L. Turnbull. 1989. The influence of simulated shadelight and daylight on growth, development and photosynthesis of *Pinus radiata, Agathis australis* and *Dacrydium cupressinum*. Plant Cell Environ. 12:343–356, doi: 10.1111/j.1365-3040.1989.tb01951.x.

Whitelam, G.C., E. Johnson, J. Peng, P. Carol, M.L. Anderson, J.S. Cowl, and N.P. Harberd. 1993. Phytochrome A null mutants of *Arabidopsis* display a wild-type phenotype in white light. Plant Cell 5:757–768, doi: 10.1105/tpc.5.7.757.

Zhang, M., Y. Park, and E.S. Runkle. 2020. Regulation of extension growth and flowering of seedlings by blue radiation and the red to far-red ratio of sole-source lighting. Scientia Hort. 272:109478, doi: 10.1016/j.scienta.2020.109478.

Supplemental Material 1. Method and Theory of Directly Measuring PPE (P_{fr}/P_{total}) in Etiolated Tissue

This method is primarily explained by Klein et al. (1967), Kendrick and Frankland (1968), and Klose (2019). The technique was modified from Butler et al. (1963).

These measurements must be made with chlorophyll-deficient tissue because chlorophyll affects the measurements, even at small concentrations. This means that either dark grown etiolated tissue or norflurazon-treated tissue must be used. Hypocotyl hooks tend to have a relatively large concentration of phytochrome and therefore this tissue is generally used for measurements. To assess the status of the major phytochrome in light grown plants, phytochrome-B, mutants are often used that are phytochrome-A deficient and phytochrome-B overexpressers (Klose et al., 2015). The tissue is packed tightly into a cuvette for measurements.

This technique requires a spectrophotometer, which measures the absorbance [or optical density (OD)] of two wavelengths simultaneously and calculates the difference between them, ΔOD. This instrument is called a dual wavelength spectrophotometer and is described in Butler et al. (1963) and Klose (2019). The two wavelengths used to calculate the ΔOD are 730 and 800 nm, such that $\Delta OD = OD_{730} - OD_{800}$. These wavelengths are chosen because the absorbance peak of P_{fr} is close to 730 nm and 800 nm is a stable reference wavelength that does not change on irradiation. Chlorophyll can still affect the readings in this region. These measurements rely on the Beer-Lampert law that states that concentration is proportional to absorbance. Therefore, ΔOD is roughly a proxy for the concentration of P_{fr}.

First, samples in the cuvettes are exposed to the photon source of interest. Then they are placed in the dark, frozen, and transported to the spectrophotometer where an initial ΔOD measurement is made, ΔOD_i. Then the sample is exposed to saturating actinic red irradiation (≈660 nm) and the ΔOD is measured again, ΔOD_R. If only P_r is absorbed at 660 nm, saturating red radiation would convert all the phytochrome to P_{fr}, and ΔOD_R would thus be a proxy for the total pool of phytochrome (P_{total}). However, that is not the case, and both P_r and P_{fr} absorb at 660 nm, so ΔOD_R must be corrected to estimate P_{total} using an estimation of PPE under saturating red photons. Many publications have calculated this value, called $X^{fr}_{red\ eq}$, φ_{660} or PPE_R. Smith and Holmes (1977) used an estimation from Pratt (1975), but this appears to be a low estimate (see Lagarias et al., 1987; Mancinelli, 1994). A good estimate of φ_{660} is 0.89.

Finally, the sample is exposed to saturating actinic FR (≈730 nm) radiation, which converts all the phytochrome to P_r, reaching a P_{fr} minimum, ΔOD_{FR}. Unlike 660 nm, which is absorbed significantly by both forms of phytochrome, 730 nm radiation is predominately absorbed by P_{fr}. P_r may cause less than 1% of the absorbance, but this error is small enough to be ignored. Therefore ΔOD_{FR} should be a proxy for a P_{fr} concentration of zero, and therefore it is treated as noise and is subtracted from both ΔOD_i and ΔOD_R as follows:

$$[P_{fr}] \propto \Delta OD_i - \Delta OD_{FR} \quad [S1.1]$$

$$[P_{total}] \propto \frac{\Delta OD_R - \Delta OD_{FR}}{\phi_{660}} \quad [S1.2]$$

Therefore, the final calculation of measured phytochrome photoequilibrium under a specific photon source uses the following equation:

$$PPE = \frac{\phi_{660} \times (\Delta OD_i - \Delta OD_{FR})}{\Delta OD_R - \Delta OD_{FR}} \quad [S1.3]$$

This technique can measure only the relative ratio of all the phytochromes (5 in *Arabidopsis* and 3 in rice), unless the use of mutants is adopted. In the main text, we say that only PPE can be measured with this technique, not [P_{fr}] or [P_{total}], but a semi-absolute measurement of P_{total} can be measured using Eq. [S1.2] if careful sample preparation is undertaken. With careful preparation in a single species, the scattering of light within the tissue can be assumed to be the same, and thus an absolute value of P_{total} can be obtained with units of ΔΔOD/mg fresh weight (Klose, 2019). However, it seems unlikely that P_{total} can be compared among species and between young and old tissue due to differences in light-scattering. This would indicate that the careful measurement of P_{total} is only a semi-absolute value.

Supplemental Material 2. Environmental Factors Impacting the Red (R) Far Red (FR) Ratio (R:FR Ratio) in Sunlight

The R:FR ratio of unfiltered sunlight varies widely and values have been reported as low as 0.7 to as high as 1.8 (Holmes and Smith, 1977a; Kotilainen et al., 2020; Salisbury, 1981; Smith, 1982, 1994). In the natural environment, water vapor, location, and the time of day also affect the R:FR ratio.

It is often thought that in full sunlight near solar noon, when the sun is at a low zenith angle (high elevation angle), the R:FR ratio is relatively constant ≈1.15 (Franklin and Whitelam, 2005; Smith, 1982), but recent data by Kotilainen et al. (2020) demonstrate the influence of atmospheric water vapor, location, and the time of day on the R:FR ratio. There is an atmospheric water vapor absorbance band with a peak at 723 nm and two oxygen absorbance bands in the R and FR region (Patadia et al., 2018; Smith, 1982) (Fig. 1). The water absorbance band depends on the amount of moisture in the atmosphere; the oxygen absorbance band is affected by length of the atmospheric path. Furthermore, light scattering through the atmosphere at low sun angles near dawn and dusk has historically been thought to significantly reduce the R:FR ratio. This has led to many end-of-day FR studies (Kasperbauer, 1971; Salisbury, 1981). More recent data indicate that low sun angles can significantly increase the R:FR ratio in some environmental conditions (Kotilainen et al., 2020). Collectively, these factors alter R:FR ratios in full sunlight in the natural environment.